PSHA Workshop, 5 to 7 September 2017, Switzerland

Earthquake-fault dip angle statistics for PSHA analyses

Roberto Basili
e-mail: *roberto.basili@ingv.it*
ORCID: *0000-0002-1213-0828*

Mara Monica Tiberti
e-mail: *mara.tiberti@ingv.it*
ORCID: *0000-0003-2504-853X*

Istituto Nazionale di Geofisica e Vulcanologia
Via Vigna Murata, 605 - 00143 Roma, Italy
www.ingv.it

Motivation

The dip angle is one of the fault parameters that most affects seismic hazard analyses because it not only influences the inference of other fault parameters (e.g. down-dip width, earthquake maximum magnitude based on fault scaling laws) but also, and most importantly, controls the fault-to-site distance values of ground motion estimates.

We present the results of a global survey of earthquake-fault dip angles (G-DIP) and analyze their empirical distribution for various faulting categories. In agreement with other studies, important deviations from the classical Anderson's predictions are found for all faulting categories.

These new empirical statistics are derived from an extended and homogeneous dataset, thereby improving previous fault dip-angle distributions. We thus suggest that our results can effectively be used as distribution priors for characterizing the geometry of poorly known seismogenic faults in seismic hazard analyses and earthquake-fault modeling experiments.

Data and preliminary assessments

G-DIP dataset

G-DIP is a collection of 217 earthquakes of Mw > 5, with univocally-determined fault plane geometry, paired with uniformly-determined moment tensor solutions from the Global CMT catalog (years 1976-2016; Dziewonski et al., 1981, and Ekström et al., 2012). The sources of the G-DIP collection are as follows:

- 18 from Sibson & Xie (1998);
- 9 from Collettini & Sibson (2001);
- 114 from SRCMOD;
- 76 from a literature search.

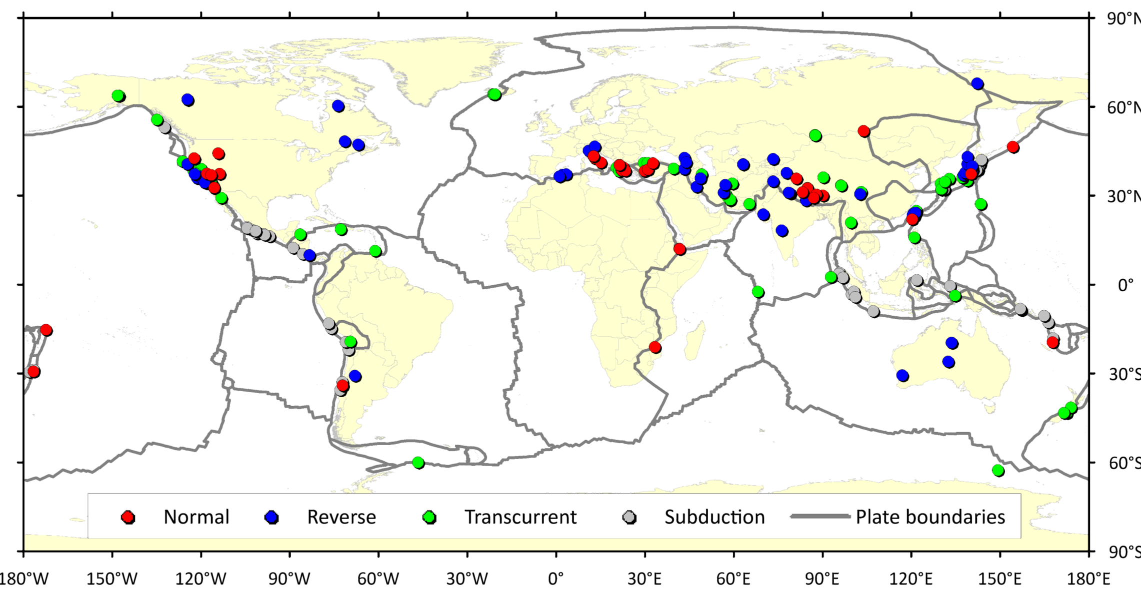

Location of the 217 G-DIP faults. Notice that this dataset includes several events from plate interiors. Plate boundaries are from Bird (2003).

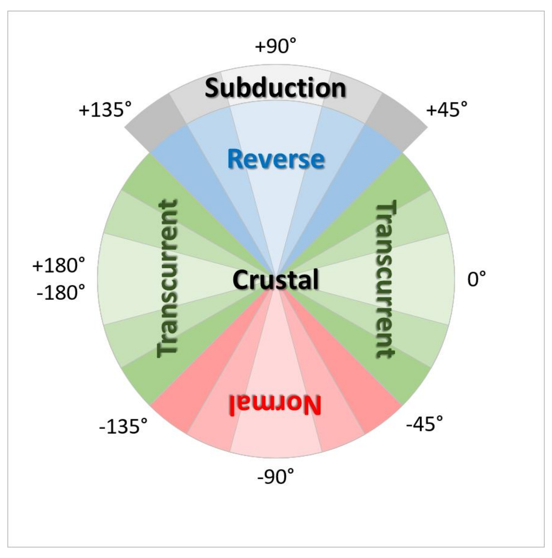

Tectonic settings

- *Crustal faulting*
- *Subduction interface faulting*

Faulting mechanisms

- *Normal*
- *Reverse*
- *Transcurrent*
- *Reverse only*

Each faulting category is further subdivided into three subsets of rake classes corresponding to intervals of ±15°, ±30°, and ±45° from the rake central values (normal: -90°; reverse: +90°; transcurrent: 0° and ±180°).

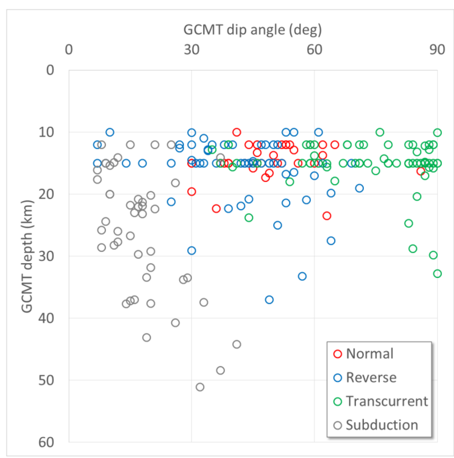

Depth of the selected events vs. the dip angle from GCMTs. The depth distribution of crustal events appears to be independent from the dip angle. In the case of subduction events the dip angle increases with increasing depth.

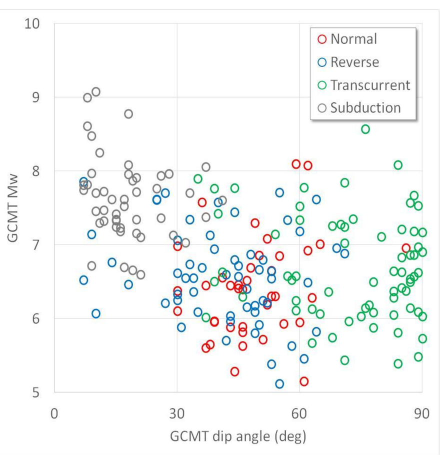

Moment magnitude (Mw) vs. the dip angle from GCMTs. The Mw distribution of crustal events appears to be independent from the dip angle.

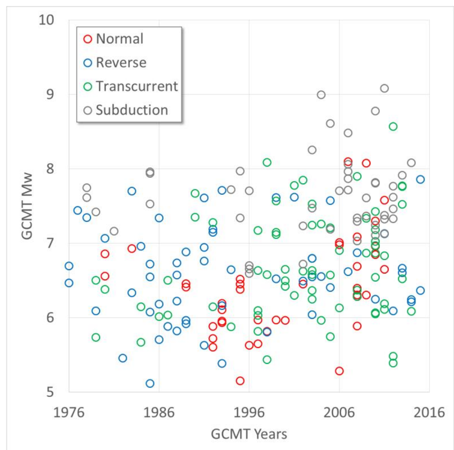

Moment magnitude (Mw) distribution through time. Notice its apparent randomness. The dataset increases in recent years thanks to the availability of more studies providing unequivocal determinations of the actual fault planes.

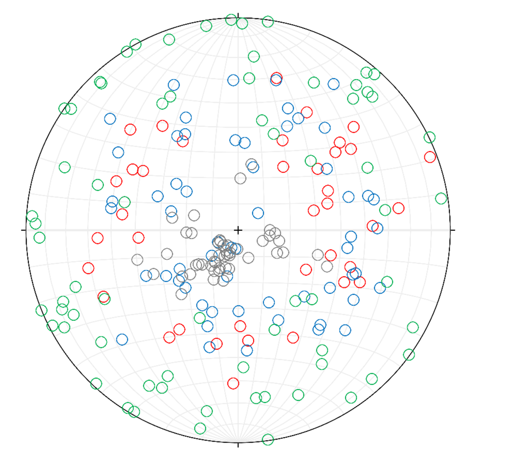

"Poles to planes" (equal area stereoplot, lower hemisphere) of the selected events from GCMTs. Only the subduction events seem to cluster around the NW-SE strike, all other types are randomly distributed.

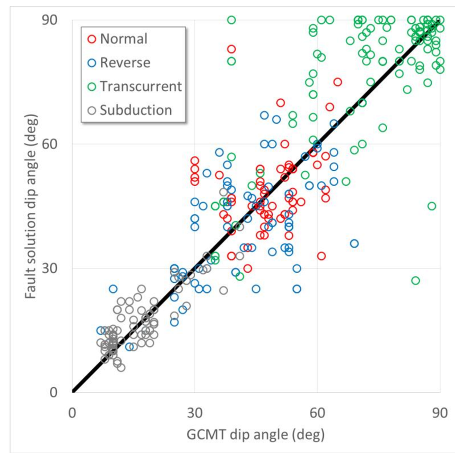

Dip angles of paired events from the GCMT catalog and from fault solutions obtained through various techniques. No bias appear between the two types of dip-angle solution.

Results

Crustal faulting			Subduction interface faulting
Normal	Reverse	Transcurrent	Reverse only

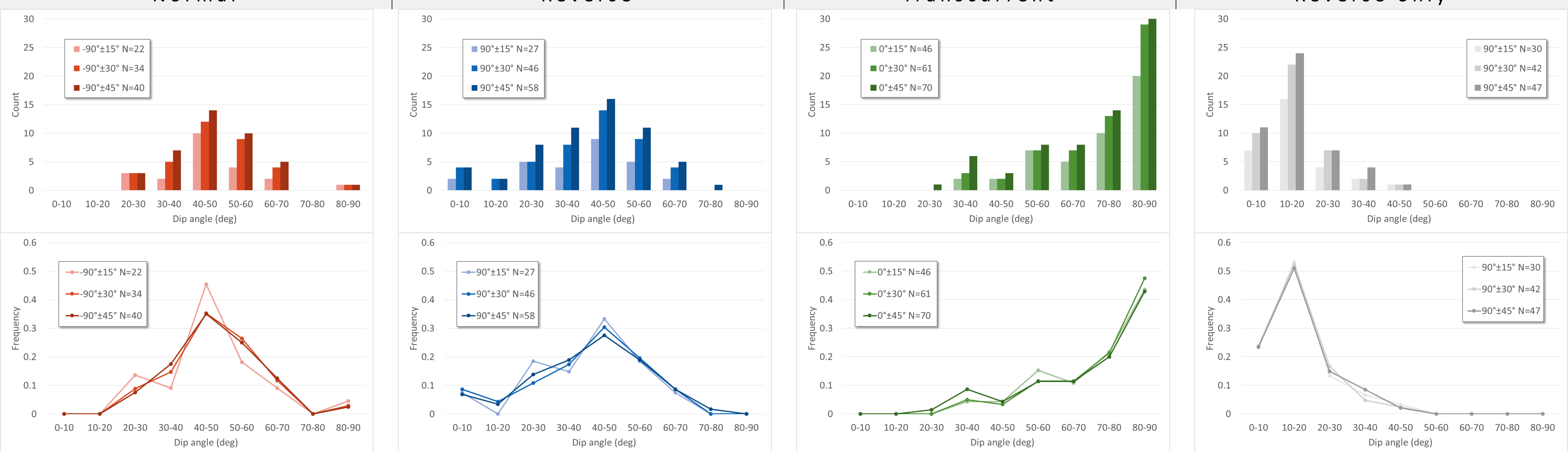

Considering the number of events in each faulting category and the uncertainty associated with angle determinations in moment tensor solutions (Helffrich, 1997), we subdivided the dip-angle domain (0-90°) in regular bins of 10°.

All distributions are unimodal. In terms of frequency of occurrence, including or excluding more oblique mechanisms (subsets with rake spanning up to ±45°) does not significantly affect the distributions.

Dip-slip faulting (normal and reverse together) shows the same mode at 40-50°, though reverse faulting has a longer tail toward lower dip angles.

Pure normal faulting (subset of -90°±15°) seems slightly more picked around the mode than the more oblique-slip normal faults.

Subduction reverse faulting shows a much picked mode (more than 50% of all events) at very low angles (10-20°) and a short tail at higher angles which is somewhat correlated with deeper events.

Transcurrent faulting has a very picked mode (slightly less than 50% of all events) at 80-90° with a very long tail.

Comparison with regional compilations of active crustal faults

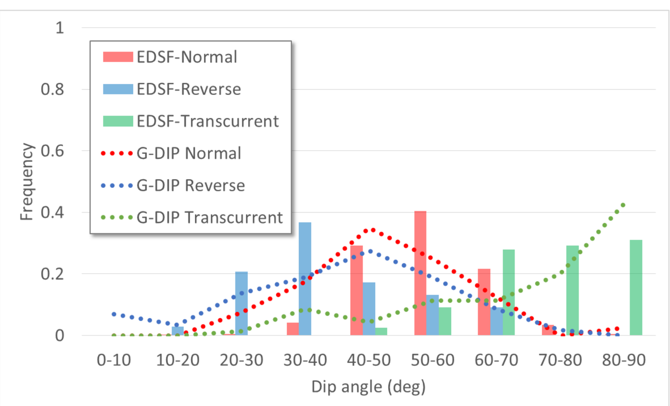

European Database of Seismogenic Faults (EDSF; Basili et al., 2013)

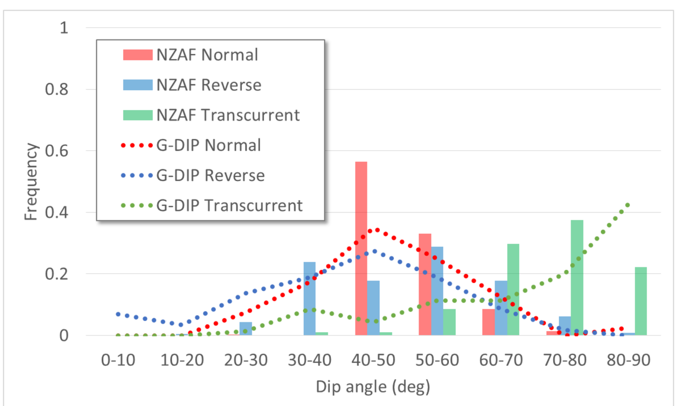

New Zealand Active Faults (NZAF; Litchfield et al., 2013).

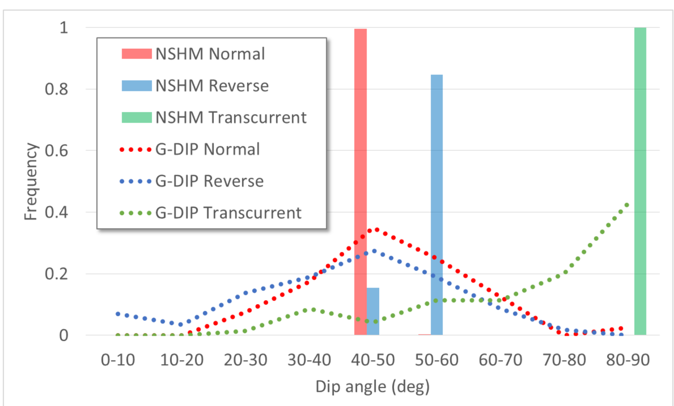

National Seismic Hazard Maps - Source Parameters (NSHM; USGS, 2014)

The occurrence of fault dip angles in three different fault datasets used in seismic hazard assessments are compared with the global distributions calculated here (subsets with rake spanning up to ±45°).

Several discrepancies between and among these distributions can be observed. Some of them may arise from the actual regional distribution of the data. However, the sources of information for estimating the dip angle of active faults are very variable, and are often available at only one or few location along the fault trace. Also, the dip angle is often inferred from fault exposures at the ground.

Despite discrepancies, the EDSF and NZAF show dip angles spanning several bins and thus seem to capture rather well the natural variability of dip angles observed at the global scale. The NSHM faults, instead, are concentrated in only one or two dip-angle bins in all three fault categories.

Acknowledgments

This work was supported by the INGV projects "Abruzzo" (code: RBAP10ZC8K_003). MMT was supported by the INGV-DPC-CPS Agreement.

We thank T. Le Pera for her help in searching the literature and constructing some data tables in an early phase of this research as part of her training.

The stereoplot was made using the software Stereonet version 9.5.3 available at http://www.geo.cornell.edu/geology/faculty/RWA/programs/stereonet.html

References

Basili, R., Kastelic, V., Demircioglu, M.B., Garcia Moreno, D., Nemser, E.S., Petricca, P., Sboras, S.P., Besana-Ostman, G.M., Cabral, J., Camelbeeck, T., Caputo, R., Danciu, L., Domac, H., Fonseca, J., García-Mayordomo, J., Giardini, D., Glavatovic, B., Gulen, L., Ince, Y., Pavlides, S., Sesetyan, K., Tarabusi, G., Tiberti, M.M., Utkucu, M., Valensise, G., Vanneste, K., Vilanova, S., Wössner, J., 2013. The European Database of Seismogenic Faults (EDSF) compiled in the framework of the Project SHARE. http://diss.rm.ingv.it/share-edsf/, doi: 10.6092/INGV.IT-SHARE-EDSF.
Bird, P., 2003. An updated digital model of plate boundaries. Geochemistry, Geophysics, Geosystems 4, n/a-n/a, doi: 10.1029/2001gc000252.
Collettini, C., Sibson, R.H., 2001. Normal faults, normal friction? Geology 29, 927-930, doi: 10.1130/0091-7613(2001)029<0927:nfnf>2.0.co;2.
Dziewonski, A.M., Chou, T.A., Woodhouse, J.H., 1981. Determination of earthquake source parameters from waveform data for studies of global and regional seismicity. Journal of Geophysical Research 86, 2825, doi: 10.1029/JB086iB04p02825.
Ekström, G., Nettles, M., Dziewoński, A.M., 2012. The global CMT project 2004–2010: Centroid-moment tensors for 13,017 earthquakes. Physics of the Earth and Planetary Interiors 200-201, 1-9, doi: 10.1016/j.pepi.2012.04.002.
Helffrich, G.R., 1997. How good are routinely determined focal mechanisms? Empirical statistics based on a comparison of Harvard, USGS and ERI moment tensors. Geophysical Journal International 131, 741-750, doi: 10.1111/j.1365-246X.1997.tb06609.x.
Litchfield, N.J., Van Dissen, R., Sutherland, R., Barnes, P.M., Cox, S.C., Norris, R., Beavan, R.J., Langridge, R., Villamor, P., Berryman, K., Stirling, M., Nicol, A., Nodder, S., Lamarche, G., Barrell, D.J.A., Pettinga, J.R., Little, T., Pondard, N., Mountjoy, J.J., Clark, K., 2013. A model of active faulting in New Zealand. New Zealand Journal of Geology and Geophysics 57, 32-56, doi: 10.1080/00288306.2013.854256.
Sibson, R.H., Xie, G., 1998. Dip Range for Intracontinental Reverse Fault Ruptures: Truth Not Stranger than Friction? Bulletin of the Seismological Society of America 88, 1014-1022.
GCMT (1976-2016) website http://www.globalcmt.org/CMTsearch.html
SRCMOD website http://equake-rc.info/SRCMOD/
USGS, 2014, National Seismic Hazard Maps - Source Parameters: Interactive Map, http://geohazards.usgs.gov/cfusion/hazfaults_2014_search/query_main.cfm.